Available online at www.sciencedirect.com
SCIENCE DIRECT®
Biochimica et Biophysica Acta xx (2006) xxx–xxx
BIOCHIMICA ET BIOPHYSICA ACTA
BBA
http://www.elsevier.com/locate/bba

Molecular mechanism of antimicrobial peptides: The origin of cooperativity

Huey W. Huang

Department of Physics and Astronomy, Rice University, Houston, TX 77251, USA

Received 2 December 2005; received in revised form 29 January 2006; accepted 1 February 2006

Abstract

Based on very extensive studies on four peptides (alamethicin, melittin, magainin and protegrin), we propose a mechanism to explain the cooperativity exhibited by the activities of antimicrobial peptides, namely, a non-linear concentration dependence characterized by a threshold and a rapid rise to saturation as the concentration exceeds the threshold. We first review the structural basis of the mechanism. Experiments showed that peptide binding to lipid bilayers creates two distinct states depending on the bound-peptide to lipid ratio P/L. For P/L below a threshold P/L^*, all of the peptide molecules are in the S state that has the following characteristics: (1) there are no pores in the membrane, (2) the axes of helical peptides are oriented parallel to the plane of membrane, and (3) the peptide causes membrane thinning in proportion to P/L. As P/L increases above P/L^*, essentially all of the excessive peptide molecules occupy the I state that has the following characteristics: (1) transmembrane pores are detected in the membrane, (2) the axes of helical peptides are perpendicular to the plane of membrane, (3) the membrane thickness remains constant for $P/L \geq P/L^*$. The free energy based on these two states agrees with the data quantitatively. The free energy also explains why lipids of positive curvature (lysoPC) facilitate and lipids of negative curvature (PE) inhibit pore formation.

Keywords: Threshold peptide concentration; Cooperative concentration dependence; Membrane thinning effect; Neutron in-plane scattering; Oriented circular dichroism; Two-state model

The interactions of antimicrobial peptides (AMP) with cells can be very complicated. (One valuable reference for AMP is the proceedings of the Ciba Foundation Symposium held in 1994 [1] which, in addition to the presentations, recorded the discussions by the pioneers of the field on wide varieties of issues pertaining to AMP research that are usually excluded from journal articles, for example, the complexities of antimicrobial activity assays.) Because AMP are strongly cationic, they can potentially bind to many anionic groups present on the cell surface. Were it not for the following two empirical findings, it would be very difficult to discuss the mechanism of AMP activity: (1) the body of evidence overwhelmingly suggests that the target site of AMP is the lipid matrix of cytoplasmic membranes [1,2] and (2) the bioactivity of AMP correlates with the leakage from lipid vesicles induced by the same AMP [1–5]. For these AMP, it is then meaningful to study their interactions with pure lipid bilayers.

Both the bio- and leakage activities induced by AMP are characterized by cooperativity (often described as all-or-none), namely, a non-linear concentration dependence characterized by a threshold and a rapid rise to saturation as the concentration exceeds the threshold [3–6]. It is important to note that this includes both the bactericidal and hemolytic activities of AMP, only that in most cases, the lethal concentrations for hemolysis are two orders of magnitude higher than that for bactericide [3,4]. This difference is understandable because AMP being cationic are attracted to the negatively charged lipids on the outer leaflets of bacterial membranes, whereas such electrostatic effect is absent for mammalian membranes, whose outer leaflets are electrically neutral. Indeed a careful analysis by Wieprecht et al. [7] showed that if the bulk peptide concentrations are replaced by surface concentrations (i.e., excluding the electrostatic effect), similar binding constants and similar threshold concentrations were obtained for neutral and negatively charged membranes. In solution, the AMP thresholds for killing microbes are in the range of micromolar, whereas the thresholds for hemolysis are in the range of hundreds of micromolar [3,4]. It is their strongly cooperative activities that make the AMP

E-mail address: hwhuang@rice.edu.

0005-2736/$ - see front matter © 2006 Elsevier B.V. All rights reserved.
doi:10.1016/j.bbamem.2006.02.001

effective antibiotics in the micromolar range without harming the host cells. Therefore, a proposed mechanism for the AMP activity must explain the origin of the cooperative concentration dependence.

The mechanism proposed below is based on very extensive studies on four peptides: alamethicin, melittin, magainin and protegrin. Although we will show only the data from our own laboratory, we will point out that our results are consistent with the data produced independently by other investigators using entirely different experimental methods and instruments.

The four peptides are among the most commonly studied due to their availability and relative simplicity. Alamethicin [8] and melittin [9] were discovered from the fungus *Trichoderma viride* and from the bee venom, respectively, in the late 1960s, and have been commercially available since 1970s. Initially, they were studied as the molecular models for voltage-gated channels (see review [10] for alamethicin, and [11] for melittin). The discoveries of AMP from animals in the 1980s, in particular magainins in the skin of *Xenopus laevis* [12], refocused the research on membrane-active peptides to their antimicrobial mechanisms [1]. Alamethicin, melittin and magainin are 20 to 26 amino acids long peptides; each forms a helical configuration when bound to lipid bilayers. The large number of studies on these peptides may have to do with the relative simplicity of their molecular structures. But it should be stressed that there is a great deal of similarities between the activity of magainins and that of cecropins from insects [3,4,12], although the latter are larger peptides and have more complex structures. This motivated us to compare helical peptides with non-helical peptides. Protegrin is an 18 amino acid peptide from the leukocytes of pigs [13]. Its configuration is a β-hairpin stabilized by two disulfide bonds. We have performed the same set of experiments on these four peptides and found that the results of all four peptides are consistent and similar to one another (references below). Thus we believe that the molecular mechanisms of cooperativity are essentially the same for these four peptides even though the details might differ.

1. Structural basis for the mechanism

1.1. Detection of pores

Do the peptides induce well-defined pores in membranes or disintegrate the membranes? To investigate this problem, we first bind peptides to lipid vesicles in various concentrations. We then evaporated most of the water, so the lipid vesicles with bound peptides flattened to become oriented multilamellae on a flat quartz surface. A simpler method for preparing such samples consists of (1) co-dissolve the lipid and peptide in an organic solvent, (2) evaporate the solvent in vacuum, (3) suspend the lipid/peptide mixture in the same solution as used for the vesicle sample, (4) lyophilize the suspension, and (5) rehydrate the lyophilized lipid/peptide mixture by water vapor. We have consistently found that the samples prepared by the two methods produced the same experimental results [14–16].

Over the years, we have experimented with a great variety of lipid compositions, including lipopolysaccharides. We found that for each peptide the threshold concentration P/L^* varies greatly with lipid compositions from below 1/200 to ~1/10 (P/L~1/200 is the detectable limit of our experimental methods). It is for experimental convenience we chose the lipid compositions that yield P/L^* within the detectable range.

Peptide-induced pores have too low an electron density contrast against the lipid background to be detected by X-ray scattering. However if we replace H_2O with D_2O, and if a pore contains a water column across the membrane, one can easily detect such water columns in a fluid membrane by neutron in-plane scattering (Fig. 1). The analysis of neutron in-plane scattering essentially yields the radius of the water column R_w and the external radius of the pore R_p (one-half of the contact distance between two pores) [17,18]. It is important to note that these neutron scattering curves have narrow widths that indicate a uniform size of pores in each sample [18]. Alamethicin

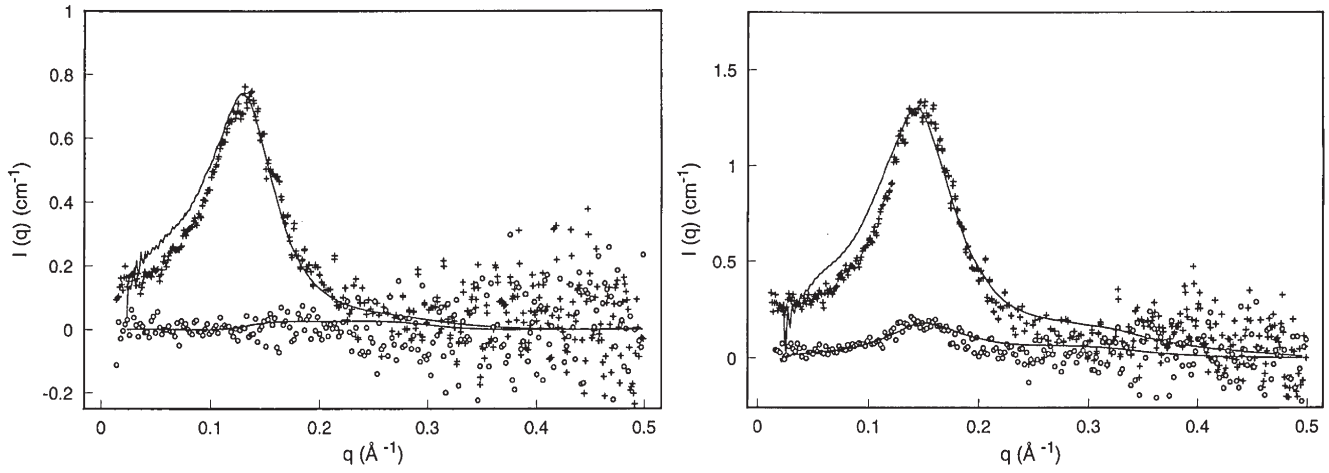

Fig. 1. Neutron in-plane scattering curve of alamethicin pores in DLPC bilayers at P/L=1/10. (Left) The data (+) were obtained when hydrated with D_2O. After the sample was exposed to H_2O vapor for 48 h, the neutron scattering curve was indistinguishable from the background (○). The solid lines are the theoretical curves of 8-monomer barrel-stave pores in D_2O or H_2O. (Right) The sample condition was the same as (Left) except that the lipid was DLPC with fully deuterated chains, hydrated with H_2O (+) or D_2O (○). The solid lines are the theoretical curves of 8-monomer barrel-stave pores (from [18]).

produced pores of $R_w \approx 9$ Å, $R_p \approx 20$ Å. These dimensions imply that the wall of the channel is 11 Å in thickness, and this is the same as the diameter of the alamethicin helix according to the crystal structures determined by Fox and Richards [19]. Thus, the alamethicin pores are consistent with the barrel-stave model [20] composed of eight alamethicin monomers (Fig. 2), in agreement with single-channel conductance measurements [21].

The pores formed by melittin [22], magainin [23–25], and protegrin [24,25] are substantially larger and with a greater size variation compared with the alamethicin pores. Their typical sizes are $R_w \approx 15$–25 Å with corresponding $R_p \approx 35$–42 Å. This size variation is from sample to sample, sensitive to the peptide, the lipid composition and sample preparations [23,24]. Like the case with alamethicin, the scattering curves of melittin, magainin and protegrin all have narrow widths that indicate a uniform size of pores in each sample. From the density of the pores in the membrane measured by neutron scattering and the peptide to lipid ratio in the sample, we estimated that only 4–7 peptide monomers in each pore [23,24]. These pores are not consistent with the barrel-stave model. Instead we proposed a toroidal model (Fig. 2) [23] for these pores, in which the lipid monolayer continuously bends from the top leaflet to the bottom leaflet through a toroidal hole, so the pore is lined by both the lipid headgroups and peptide monomers. The peptides are embedded among the lipid headgroups as in the case of surface adsorption, essentially serving as fillers in the headgroup region of the curved lipid monolayer so as to relieve the bending stress [23]. A similar pore model was independently proposed by Matsuzaki's group based on their fluorescence and leakage experiments [26]. Unlike the barrel-stave model where the peptide needs to be long enough to span the membrane, the toroidal model can be induced by smaller peptides because here the peptides probably play the role of stabilizing the lipid pore rather than lining the pore.

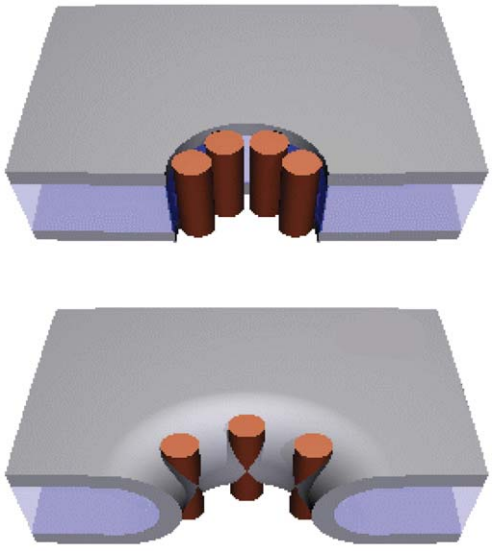

Fig. 2. Schematics of the barrel-stave model (top) and the toroidal model (bottom). The dark layers represent the headgroup regions of bilayers. Peptide monomers are represented by the cylinders (From [22]).

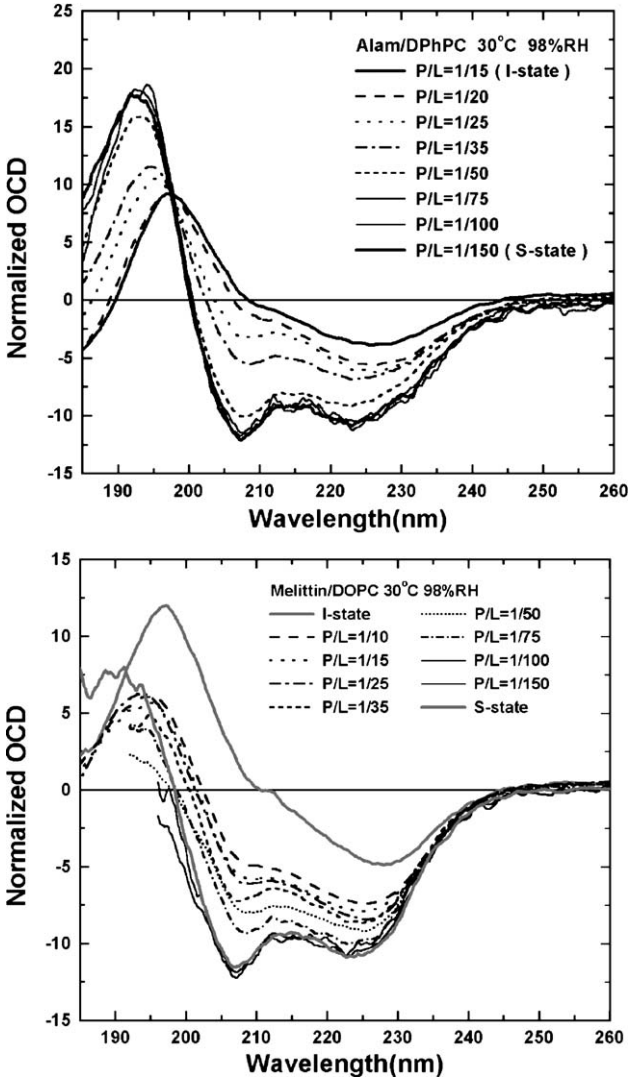

Fig. 3. (Top) OCD spectra of alamethicin in DPhPC bilayers with *P/L* varied from 1/150 to 1/15. The spectra of *P/L*=1/150 and 1/15 are the spectra for the S state and the I state of alamethicin, respectively. All other spectra are each a linear combination of S and I. (Bottom) OCD of melittin in DOPC bilayers with *P/L* varied from 1/150 to 1/10. The high UV absorptance by DOPC made the spectra below ~200 nm unacceptably noisy. The spectra I and S of melittin were established in [22]. All spectra are each a linear combination of S and I (from [35]).

1.2. Orientation of peptide

We have developed a method of oriented circular dichroism (OCD) [27,28] to measure the orientation of peptides in membranes, first for helical peptides [27,28], then for β-sheet peptides [29] and for cyclic peptides [30]. The merit of this method is in its speed of measurement; it often takes only several minutes per sample. This allowed us to measure the peptide orientation in a wide range of sample conditions that led us to discover the rotation of peptide orientation as a function of concentration [31].

Peptide orientation was measured by OCD as a function of the bound-peptide to lipid molar ratio (*P/L*) in each case (Fig. 3), using the same sample preparation as for neutron

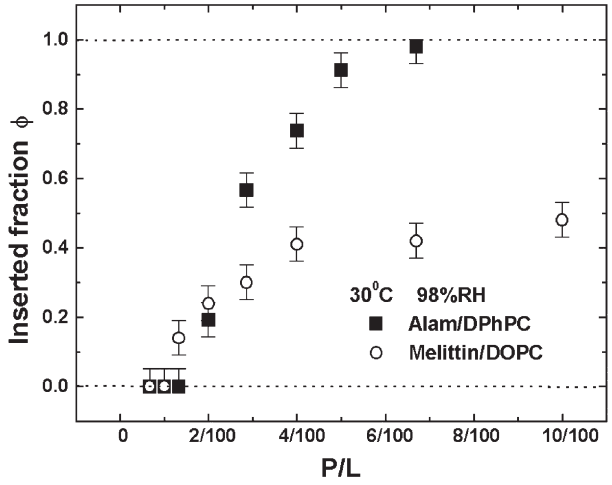

Fig. 4. Fraction of peptide molecules occupying the I state, ϕ, obtained from Fig. 3 is plotted as a function of peptide concentration *P/L*: (solid square) alamethicin in DPhPC and (open circle) melittin in DOPC (from [35]).

experiment. In all cases, we found that at low concentrations the peptide orientation indicate surface binding, defined as the S state. However as the peptide concentration *P/L* increases, there is a threshold *P/L** above which an increasing fraction of the peptide monomers change to another orientation, defined as the I state ([31] for alamethicin, [22] for melittin, [15] for magainin, [29] for protegrin). In the case of helical peptides, the S state corresponds to the helical axis oriented parallel to the plane of the bilayer. When the concentration exceeds *P/L**, a fraction of the peptide monomers change to the I state, corresponding to the helical axis oriented perpendicular to the plane of the bilayer (Fig. 4). The value of the threshold *P/L** depends on the peptide as well as the lipid composition of the bilayer. (The β-sheet peptide protegrin exhibits a characteristic OCD at low P/L and another characteristic OCD at high P/L, entirely parallel to the behaviors of helical peptides [29]. However, the theoretical interpretation of the OCD in terms of the β-sheet orientation is not available.)

An important advantage of the OCD method is that the same identical sample for OCD measurement can be subject to neutron experiment. We have repeatedly found this important correlation between OCD and neutron experiments, namely, when OCD showed that all the peptides were in the S state, neutron scattering showed no pores present in the membrane; on the other hand, neutron scattering showed the presence of pores when OCD showed a detectable fraction of the peptide in the I state, [18,22]. (Note that one can also reversibly change the peptide orientation by placing the sample in a humidity chamber and vary the degree of hydration or the temperature of the sample [22,29,31]. A sample of fixed *P/L* can exist in either the S state or the I state by varying the hydration or temperature, and the correlation test has been done on both states of the same sample [18,22].) Thus, we could identify the state of pores as the I state.

1.3. Membrane thinning effect

The oriented multilayers of peptide–lipid mixtures were also measured by X-ray diffraction. In the neutron in-plane

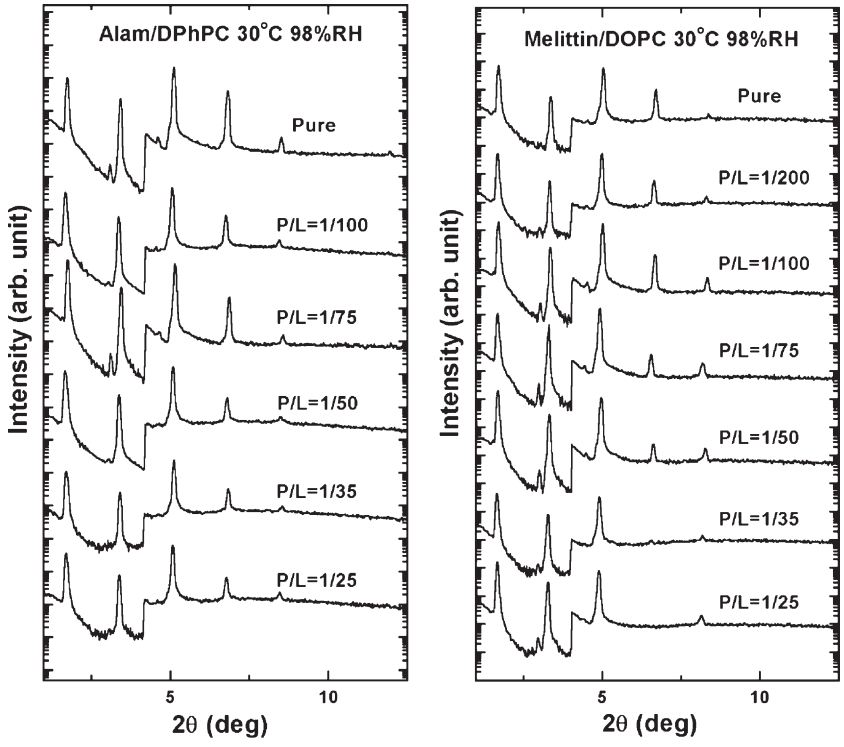

Fig. 5. X-ray diffraction patterns of pure DPhPC and DPhPC containing alamethicin at various *P/L* (left), and of pure DOPC and DOPC containing melittin at various *P/L* (right). The patterns are displaced for clarity. The steps at 2θ ~4° were due to the use of an X-ray attenuator to reduce the count rates for the first two diffraction orders in order not to saturate the detector (from [35]).

scattering we oriented the scattering vector parallel to the plane of the bilayers to study the in-plane structures. Here, we oriented the X-ray scattering vector perpendicular to the plane of the bilayers to measure the electron density profile across the membrane (Fig. 5). The one parameter that can be measured very precisely by this method is the membrane thickness or, more specifically, the distance between the two phosphate groups across the bilayer (Fig. 6). It has been noted in all such measurements, peptide reduces the membrane thickness in proportion to *P/L* ([32] for alamethicin, [33] for magainin, [34] for protegrin, [35] for melittin).

More systematic measurements over a wide range of *P/L* showed that the membrane thickness decreases linearly with *P/L* until it reaches a threshold, thereafter the thickness remains constant as *P/L* further increases. Most strikingly, this threshold is coincidental with the threshold concentration for the peptide orientation change as measured by OCD (Fig. 6).

1.3.1. Two-state model

Thus, we have seen three independent measurements all showing a common threshold concentration *P/L**. For peptide concentrations below *P/L**, all of the peptide molecules are in the S state that has the following characteristics: (1) there are no pores in the membrane, (2) the axes of helical peptides are oriented parallel to the plane of membrane, and (3) the peptide causes membrane thinning in proportion to *P/L*. As the peptide concentration increases above *P/L**, an increasing fraction of the peptide molecules occupy the I state that has the following characteristics: (1) transmembrane pores are detected in the membrane, (2) the axes of helical peptides are perpendicular to the plane of membrane, (3) the membrane thickness remains constant for $P/L \geq P/L^*$. This two-state model, first reviewed in [36], is depicted in Fig. 7.

In a vesicle experiment performed by Longo et al. [37], the membrane area was monitored by micropipette aspiration. Also, by use of solutes of different size within and outside vesicles, membrane permeation was detected by the swelling resulting from unidirectional flux of solute and co-transport of water. When the vesicle was exposed to melittin at low concentrations, the vesicle membrane area expanded with no change in the vesicle volume, consistent with the peptide molecules bound to the vesicle in the S state. When the vesicle was exposed to melittin at high concentrations, initially, the vesicle membrane area expanded with no change in the vesicle volume, but

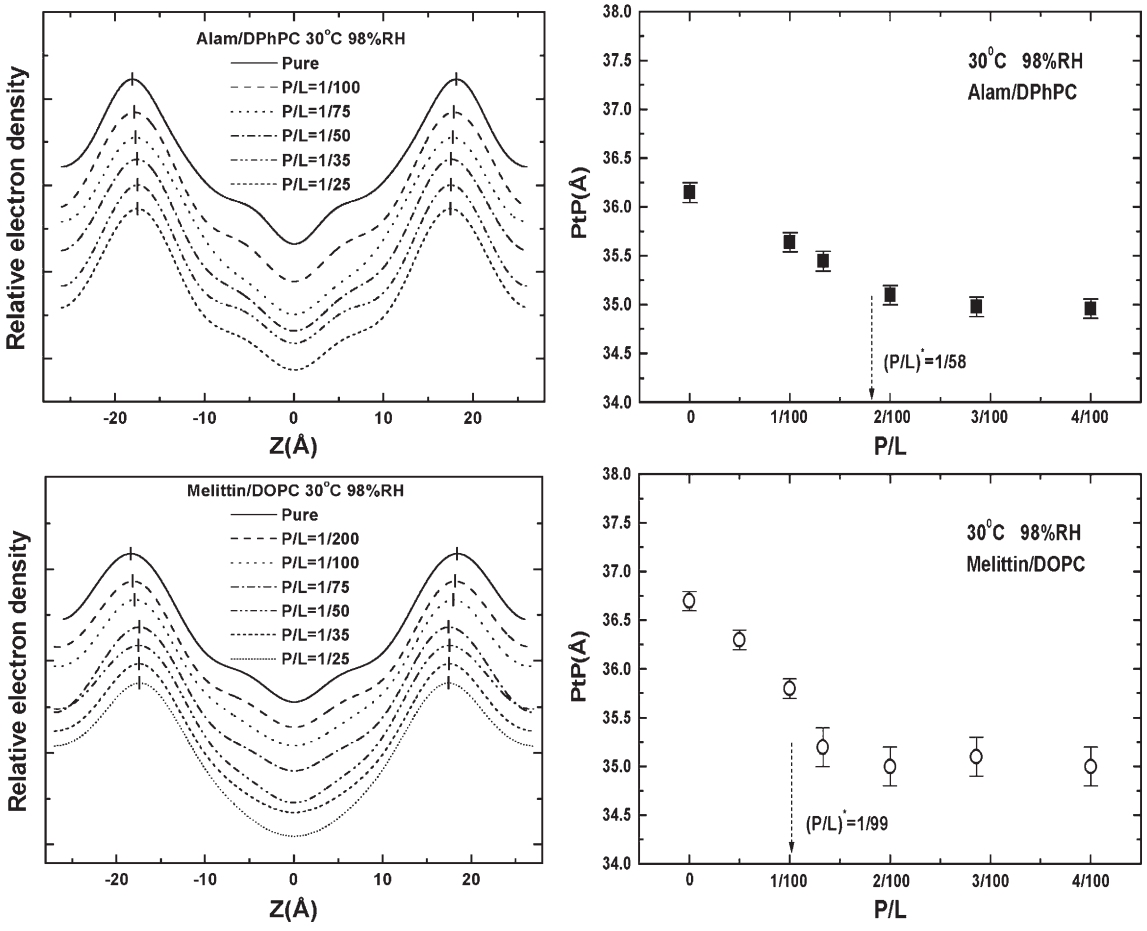

Fig. 6. (Left) Electron density profiles of pure DPhPC and DPhPC containing alamethicin at various *P/L* (top), and of pure DOPC and DOPC containing melittin at various *P/L* (bottom). The profiles are displaced for clarity. The short vertical bars indicate the positions of the peaks. (Right) Peak-to-peak distance (*PtP*) vs. *P/L* for DPhPC containing alamethicin (top) and DOPC containing melittin (bottom). In each panel, the arrow indicates (*P/L*)*, the onset of S-to-I transition measured by OCD (see Fig. 4). *PtP* decreases linearly with *P/L* below (*P/L*)*. Above (*P/L*)*, the *PtP* is constant within experimental errors (from [35]).

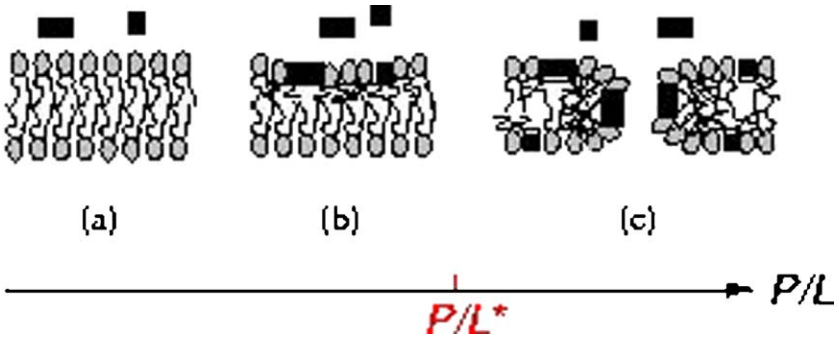

Fig. 7. Two-state Model. The black rectangles represent helical peptides viewed either along the helix or sideways. (a) Before peptide binding; (b) peptides are bound to the lipid bilayer in the S state for $P/L < P/L^*$; (c) for $P/L > P/L^*$, a fraction of peptide molecules form pores (the I state) (from [54]).

subsequently the vesicle volume increased indicating that pores were formed in the membrane that allowed permeation of small solute molecules but not the large ones. This experiment was entirely consistent with the two-state model described above.

The membrane thinning effect implies that the membrane area is expanded by peptide binding. Specifically the peptide in the S state is bound to the interface, embedded between the headgroups rather than on the top of the headgroups. This was confirmed by other probing methods, in particular fluorescence [38] and solid-state NMR [39–42]. When a peptide molecule is bound to the interface, it creates a gap underneath that is filled by the surrounding chains. This causes a local thinning or a dimple (Fig. 8) [33]. The energy of this deformation and the range of deformation have been calculated [43] by use of an elasticity theory characterized by an area stretch modulus K_A [44] and a bending rigidity K_C [45]. The persistence length of deformation $\xi=(16h^2K_C/K_A)^{1/4}$ (where h is the hydrocarbon thickness) is 20–40 Å, depending on the values of the elastic constants. There are several theoretical consequences that are relevant to the experimental observations here. According to the theory, two dimple deformations are repulsive to each other within a distance $\sim 2\sqrt{2\xi}$ (slightly attractive beyond this distance) [43]. This means that the peptide molecules in the S state ought to be monomers and dispersed on the membrane surface, consistent with the solid-state NMR observations [41,42]. This is contrary to a rather common speculation that peptide molecules may aggregate or associate on the membrane surface as a prelude to pore formations. In fact many fluorescence energy transfer experiments [46–48] designed to look for peptide aggregation did not find either aggregation or association of peptides in the S state.

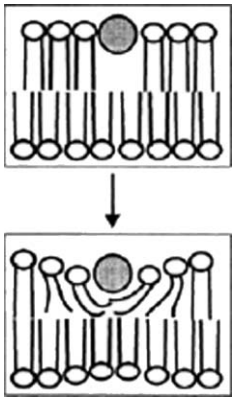

Fig. 8. A peptide molecule binding to the interface would force a gap in the chain region (top). For this gap to be filled, the chains must become locally thinner (bottom) (from [33]).

The key for understanding the mechanism of the peptides is to note that although an individual peptide molecule binds to the interface with a negative binding energy $-\varepsilon_s$ due to hydrophobic interaction, the binding incurs a positive energy of elastic deformation (the dimple energy $F^{(1)}$). At low P/L, when the dimple deformations of individual peptide molecules do not overlap, the total deformation energy is proportional to $(P/L)F^{(1)}$. The theory showed that when P/L is sufficiently high, so that the dimple deformations of individual peptide molecules substantially overlap, the total deformation energy becomes proportional to $(P/L)^2F^{(1)}$ [43]. Thus the energy level of the S state contains a positive term that increases with P/L, so that the energy level of the S state will eventually catch up with the energy level of pore formation ($-\varepsilon_p$) when P/L is sufficiently large. Once P/L reaches this threshold, any more peptide molecule binding to the membrane will go to the I state and form pores (because if the peptide goes to the S state, its energy would become higher than that of the I state). This qualitatively explains the transition from the S state to the I state as a function of P/L.

1.3.2. Free energy of the mechanism

The energy calculation becomes simple at sufficiently high P/L when the dimple deformations by individual peptide molecules overlap and the membrane thickness becomes approximately uniform. We express the membrane area increase by $\Delta A/A=A_PP/A_LL$ where A_P is defined as the area increase by one peptide in the S state and A_L is the cross sectional area per lipid. The conservation of chain volume implies $\Delta A/A=-\Delta h/h$ where the thickness of the hydrocarbon region h is $PtP-10$ Å, or PtP minus twice the length of the glycerol region (from the phosphate to the first methylene of the hydrocarbon chains); the latter is very close to 10 Å [49–51]. $-\Delta h/h$ or $\Delta A/A$ is directly measured by X-ray diffraction (Fig. 6).

It is convenient to consider an equivalent tension σ associated with the area expansion: $\sigma=K_A\Delta A/A=K_A|\Delta h/h|$ [52]. Then the differential free energy change in the S state for a small change in the number of bound peptide molecules δP is

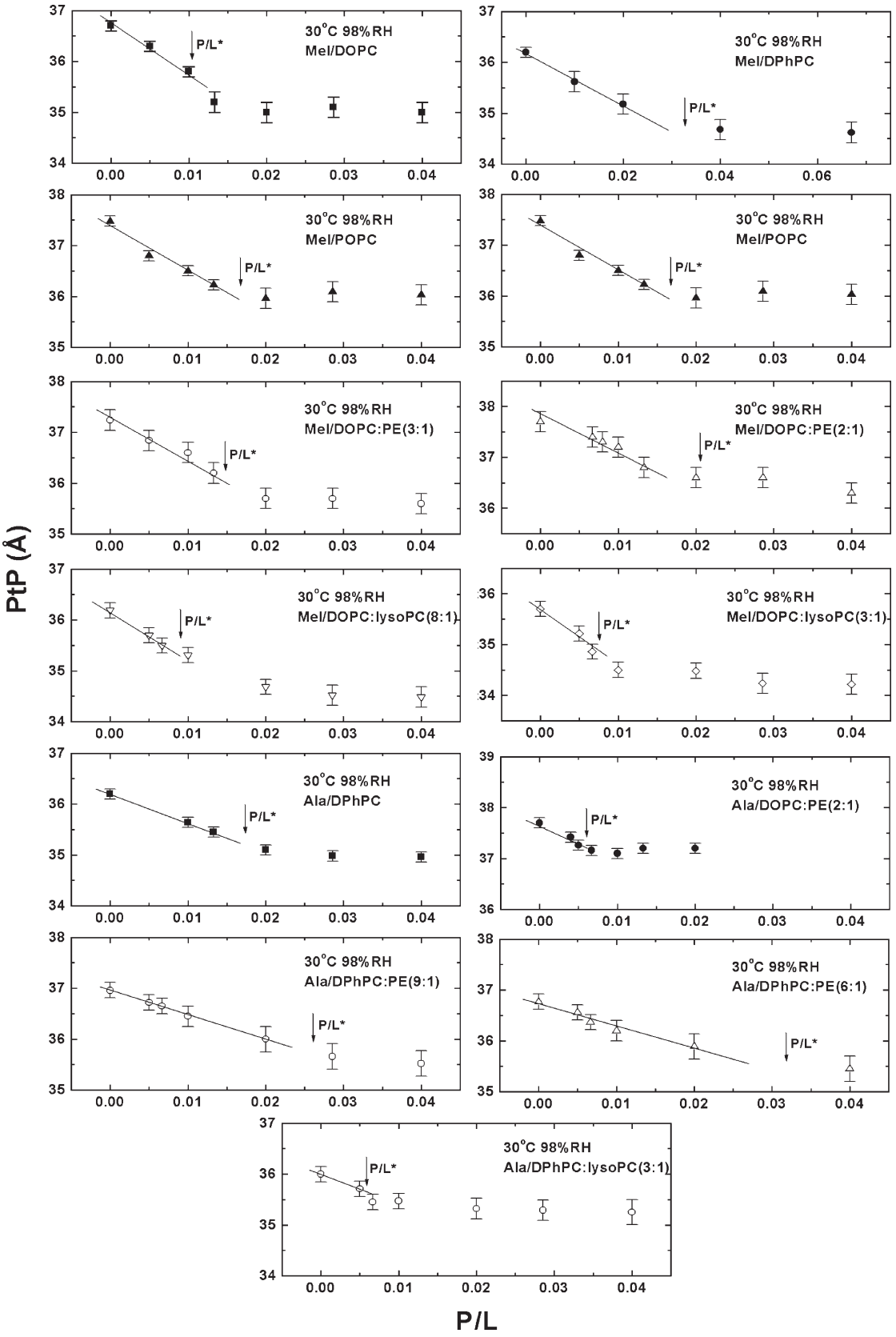

Fig. 9. Peak-to-peak distance (*PtP*) of lipid bilayer as a function of peptide concentration *P/L*. Each panel shows a different peptide/lipid combination. The corresponding threshold concentration *P/L** measured by OCD is indicated in each panel. In each case, *PtP* decreases linearly with *P/L* until it reaches a plateau. The beginning of the plateau is very close to the *P/L** measured by OCD. The data are collected from [35,52,54,56].

$\delta F = -\varepsilon_s \delta P + \sigma \delta A$. For a finite (rather than infinitesimal) P/L, the free energy change in the S state normalized to per lipid is:

$$\Delta F/L = \Delta f = -\varepsilon_s(P/L) + (1/2)K_A A_L(\Delta A/A)^2 = -\varepsilon_s(P/L) + (1/2)K_A(A_P^2/A_L)(P/L)^2 \quad (1)$$

For $P/L > P/L^*$, a fraction ϕ of the bound peptide molecules, $\phi P \equiv P_I$, participates in pore formation. We have to allow for a possible effect of the pore on the membrane thickness. Thus we modify $\Delta A = A_P P$ for $P/L < P/L^*$ to

$$\Delta A = A_P(P - P_I) + \beta A_P P_I \quad (2)$$

for $P/L > P/L^*$. The parameter β expresses the effect of pore-participating peptides relative to the effect of surface bound peptides. For example, if $\beta = 1$, the pores have the same effect of thinning as if the pore-participating peptides were on the surface, and if $\beta = 0$, the pores have no effect on the membrane thickness. Then, for $P/L > P/L^*$, the free energy change is given by [35,53,54]:

$$\Delta f = -\varepsilon_s(1-\phi)(P/L) - \varepsilon_p \phi P/L + (1/2)K_A(A_P^2/A_L)[(1-\phi)P/L + \beta\phi P/L]^2.$$

Minimization of Δf with respect to ϕ, i.e., $\partial \Delta f / \partial \phi = 0$, has two theoretical consequences or predictions: (1) The membrane thickness is constant for $P/L \geq P/L^*$. Fig. 9 shows a large number of measurements confirming this prediction. (2) The result of $\partial \Delta f / \Delta \phi = 0$ can be rearranged to:

$$\phi = \frac{1}{1-\beta}\left(1 - \frac{P/L^*}{P/L}\right) \quad (4)$$

where the threshold concentration is given by

$$P/L^* = \frac{\varepsilon_s - \varepsilon_p}{K_A(A_P^2/A_L)(1-\beta)}. \quad (5)$$

Eq. (4) predicts that ϕ is linear with respect to the reciprocal of P/L. This is also confirmed by a large number of measurements collected in Fig. 10.

All the parameters in the free energy Eq. (3) can be measured by combination of the membrane thinning experiment and the peptide orientation experiment. Some examples are shown in Table 1 [54].

1.3.3. The lipid dependence

The most conspicuous lipid dependence is that of charged lipids versus neutral lipids. As mentioned in the Introduction, this electrostatic effect mainly affects the initial binding of peptides to membranes [7]. However, even after the initial binding is normalized, that is, if the vesicle leakage experiment is expressed as a function of the bound-peptide to lipid ratio P/L, there is still noticeable lipid dependence. In two leakage experiments with magainin [6] and melittin [55], it was found that addition of PE to the lipid composition of the vesicles increased the peptide threshold concentration for pore formation, whereas addition of lysoPC decreased the threshold concentration. This appears to correlate with the mean positive curvature of a toroidal pore, namely, lipids of positive curvature (lysoPC) facilitate and lipids of negative curvature (PE) inhibit pore formation. Thus, the correlations were taken as evidence supporting the toroidal model for magainin and melittin [6,55]. We have investigated these correlations systematically and found the root of the lipid dependence lying somewhere else.

We have added lysoPC and PE to both alamethicin and melittin systems and found that in both cases, lysoPC facilitates and PE inhibits pore formation (Table 2 [56]). Thus this lipid dependence is not unique to toroidal pores. The formula for P/L^* (Eq. (5)) allows us to analyze the lipid dependence more quantitatively. There are three factors: $(\varepsilon_s - \varepsilon_p)$, $1/K_A(A_P^2/A_L)$ and $1/(1-\beta)$ in Eq. (5). In Fig. 11, we plotted the variation of the threshold P/L^* against the variation of the factor $1/K_A(A_P^2/A_L)$, and found an approximately one-to-one correlation for both alamethicin and melittin. In other words, the dominating factor for the lipid dependence is $1/K_A(A_P^2/A_L)$. Since the stretch moduli K_A are nearly the same for all lipids [44], the key factor is (A_P^2/A_L).

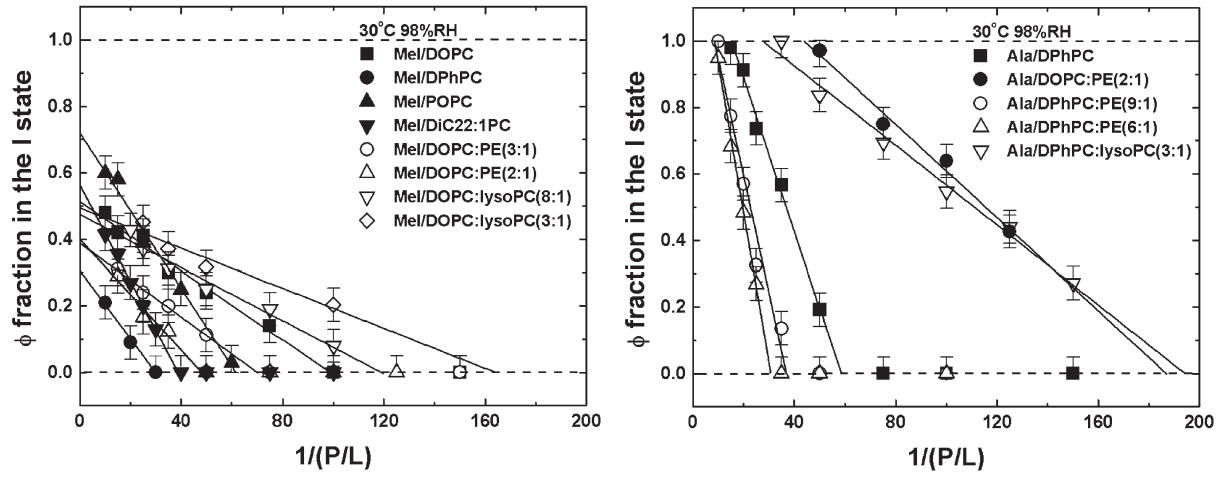

Fig. 10. The fraction of peptide molecules in the I state is plotted against $1/(P/L)$. In each case, the data for P/L above P/L^* fall into a straight line in agreement with the prediction by Eq. (4). The data are collected from [35,53,54,56].

Table 1
Experimental parameters of peptide–lipid interaction pertinent to the mechanism of pore formation [54]

Peptide	Melittin				Alamethicin	
Lipid	DPhPC	DOPC	DiC22:1PC	POPC	DPhPC	DOPC: PE(2:1)
K_A (pN/nm)	240					
h (Å)	26.2	26.6	35.1	27.5	26.2	27.7
A_L (Å^2)	91	74	69	68	91	71
A_P (Å^2)	175	246	237	223	193	208
P/L*	1/30	1/99	1/39	1/62	1/58	1/187
β	−2.27	−0.95	−0.77	−0.39	0.24	0.24
$\varepsilon_s-\varepsilon_p$ (kcal/mol)	12.7	5.6	12.8	5.7	1.9	0.9
σ* (pN/nm)	15.4	8.0	20.5	12.7	8.8	3.8

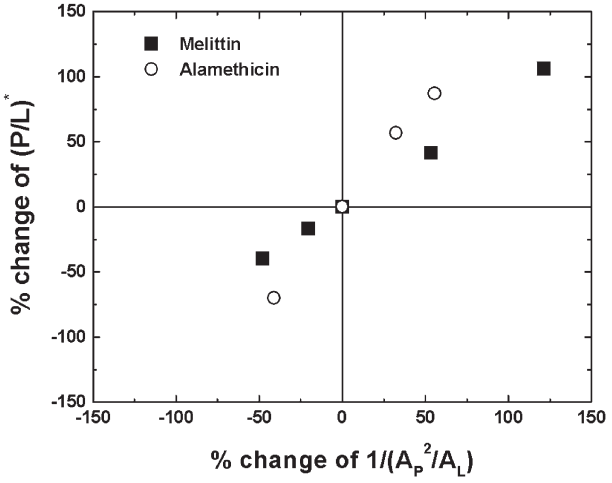

Fig. 11. Correlation between the threshold concentration P/L* and the thinning effect. Melittin in pure DOPC and alamethicin in pure DPhPC are taken as the reference (central) point. The percent change of P/L* is plotted against the percent change of the factor $1/(A_P^2/A_L)$ as a result of adding PE or lysoPC to the pure PC bilayers. Note that in both cases, the slopes of the data points are close to 45° or one-to-one correlations (from [56]).

At first sight, this is puzzling–A_P, defined as the area expansion of the lipid monolayer per peptide binding, seems to represent the physical cross section of the peptide molecule, yet it varies greatly with lipid composition (Tables 1, 2). We believe that this is because peptide binding releases some water molecules from the headgroup region—the water release reduces the area expansion [54,57]. That explains why the value of A_P is always less than the physical cross section of the peptide molecule [54,56]. Because of the size differential between the headgroup and chains cross sections, there are more water molecules in PE headgroups than in PC headgroups, and conversely for lysoPC. Peptide binding releases more water molecules from PE headgroups than it does from PC headgroups. Accordingly A_P decreases with the addition of PE but increases with the addition of lysoPC. Since the value of A_P measures the effect of a peptide in expanding the membrane area or thinning the membrane that drives the membrane toward creating pores, the lipid dependence of A_P largely reflects the lipid dependence of the peptide activity.

How about the effect of lipid curvature on the energy of pore formation? This effect is in the factor $(\varepsilon_s-\varepsilon_p)$. As we can see in Table 2, there is no systematic change in $(\varepsilon_s-\varepsilon_p)$ by the addition of PE or lysoPC. The argument that the lipid curvature should affect the energy of toroidal pore assumes that there is a bending stress in the pore formation. Perhaps the bending stress has already been diminished by the participation of peptides in the pore.

2. Concluding remark

The mechanism presented above is general. It requires only the amphipathic property of the peptides that makes the molecules favorable to bind to the interface of lipid bilayers. A peptide binding causes a local membrane area expansion and therefore an equivalent local tension. It is well known that pore formation occur spontaneously in a pure lipid vesicle if the latter is under tension [58–60]. It is instructive to note that the equivalent tension at the threshold concentration for pore formation $\sigma^*=K_A(A_P/A_L)(P/L^*)$ (8.0 pN/nm in DOPC [54]) is in agreement with the rupture tension of the vesicles made of the same lipid composition (9.9±2.6 pN/nm for pure DOPC [61]).

We understand that even at extremely low concentrations, antimicrobial peptides can induce, by fluctuations, transient pores that allow ion conduction but not leakage of large molecules [1,62]. (Transient pores would also allow

Table 2
Effects of adding PE or LysoPC [56]

Peptide	Melittin					Alamethicin			
Lipid	DOPC: LysoPC (3:1)	DOPC: LysoPC (8:1)	DOPC	DOPC: DOPE (3:1)	DOPC: DOPE (2:1)	DPhPC: LysoPC (3:1)	DPhPC	DPhPC: DPhPE (9:1)	DPhPC: DPhPE (6:1)
h (Å)	25.7	26	26.6	27.2	27.7	26	26.2	27	26.8
A_L (Å^2)	67	71.5	74	72	71	78	91	88	89
A_P (Å^2)	324	271	246	196	162	233	193	165	153
P/L*	1/164	1/119	1/99	1/70	1/48	1/194	1/58	1/37	1/31
β	−1.02	−1.11	−0.95	−1.57	−1.5	0.14	0.24	0.23	0.26
$\varepsilon_s-\varepsilon_p$ (kcal/mol)	6.7	6.3	5.6	6.8	6.7	1.1	1.9	2.2	2.2

translocation of peptides between two leaflets [26]). Stable pores appear only when the peptide concentration exceeds a threshold. (Pores are stable in the sense that there is a well defined density of pores as detected by neutron scattering, even though individual pores probably form and dissociate reversibly.) Qualitatively, the origin of cooperativity can be understood as follows: there are no stable pores that cause leakage at peptide concentrations below the threshold. But once the concentration exceeds the threshold, essentially all of the excessive peptide molecules form stable pores.

Acknowledgements

This work was supported by NIH Grant GM55203 and the Robert A. Welch Foundation Grant C-0991.

References

[1] H.G. Boman, J. Marsh, J.A. Goode (Eds.), Antimicrobial Peptides, Ciba Foundation Symposium, vol. 186John Wiley and Sons, Chichester, 1994.
[2] M. Zasloff, Antimicrobial peptides of multicellular organisms, Nature 415 (2002) 389–395.
[3] R.B. Merrifield, E.L. Merrifield, P. Juvvadi, D. Andreu, H.G. Boman, Design and synthesis of antimicrobial peptides, in Ref. [1], pp. 5–26.
[4] H. Steiner, D. Ardreu, R.B. Merrifield, Binding and action of cecropins and cecropins analogs: antimicrobial peptides from insects, Biochim. Biophys. Acta 939 (1988) 260–266.
[5] Y. Pouny, D. Rapaport, A. Mor, P. Nicolas, Y. Shai, Interaction of antimicrobial dermaseptin and its fluorescently labeled analogs with phospholipid membranes, Biochemistry 31 (1992) 12416–12423.
[6] K. Matsuzaki, K. Sugishita, N. Ishibe, M. Ueha, S. Nakata, K. Miyajima, R.M. Epand, Relationship of membrane curvature to the formation of pores by magainin 2, Biochemistry 37 (1998) 11856–11863.
[7] T. Wieprecht, O. Apostolov, M. Beyermann, J. Seelig, Membrane binding and pore formation of the antimicrobial peptide PGLa: thermodynamic and mechanistic aspects, Biochemistry 39 (2000) 442–452.
[8] P. Meyer, F. Reusser, A polypeptide antibacterial agent isolated from *Trichoderma viride*, Experientia 23 (1967) 85–86.
[9] E. Habermann, J. Jentsch, Sequenzanalyse des Melittins aus seinen tryptischen und peptischen Spaltstucken, Hoppe-Seyler Z. Physiol. Chem. 348 (1967) 37–50.
[10] R. Latorre, O. Alvarez, Voltage-dependent channels in plannar lipid bilayer membranes, Physiol. Rev. 61 (1981) 77–150.
[11] M.T. Tosteson, D.C. Tosteson, The sting: melittin forms channels in lipid bilayers, Biophys. J. 36 (1981) 109–116.
[12] M. Zasloff, Magainins, a class of antimicrobial peptides from *Xenopus* skin: isolation, characterization of two active forms, and partial cDNA sequence of a precursor, Proc. Natl. Acad. Sci. U. S. A. 84 (1987) 5449–5453.
[13] V.N. Kokryakov, S.S.L. Harwig, E.A. Panyutich, A.A. Shevchenko, G.M. Aleshina, O.V. Shamova, H.A. Korneva, R.I. Lehrer, Protegrins: leukocyte antimicrobial peptides that combine features of corticostatic defensins and tachyplesins, FEBS Lett. 327 (1993) 231–236.
[14] H.W. Huang, G.A. Olah, Uniformly oriented gramicidin channels embedded in thick monodomain lecithin multilayers, Biophys. J. 51 (1987) 989–992.
[15] S.J. Ludtke, K. He, Y. Wu, H.W. Huang, Cooperative membrane insertion of magainin correlated with its cytolytic activity, Biochim. Biophys. Acta 1190 (1994) 181–184.
[16] L. Ding, L. Yang, T.M. Weiss, A.J. Waring, R.I. Lehrer, H.W. Huang, Interaction of antimicrobial peptides with lipopolysaccharides, Biochemistry 42 (2003) 12251–12259.
[17] K. He, S.J. Ludtke, D.L. Worcester, H.W. Huang, Antimicrobial peptide pores in membranes detected by neutron in-plane scattering, Biochemistry 34 (1995) 15614–15618.
[18] K. He, S.J. Ludtke, D.L. Worcester, H.W. Huang, Neutron scattering in the plane of membrane: structure of alamethicin pores, Biophys. J. 70 (1996) 2659–2666.
[19] R.O. Fox, F.M. Richards, A voltage-gated ion channel model inferred from the crystal structure of alamethicin at 1.5-Å resolution, Nature 300 (1982) 325–330.
[20] G. Baumann, P. Mueller, A molecular model of membrane excitability, J. Supramol. Struct. 2 (1974) 538–557.
[21] D.D. Mak, W.W. Webb, Two classes of alamethicin transmembrane channels: molecular models form single-channel properties, Biophys. J. 69 (1995) 2323–2336.
[22] L. Yang, T.A. Harroun, T.M. Weiss, L. Ding, H.W. Huang, Barrel-stave model or toroidal model? a case study on melittin pores, Biophys. J. 81 (2001) 1475–1485.
[23] S.J. Ludtke, K. He, W.T. Heller, T.A. Harroun, L. Yang, H.W. Huang, Membrane pores induced by magainin, Biochemistry 35 (1996) 13723–13728.
[24] L. Yang, T.M. Weiss, T.A. Harroun, W.T. Heller, H.W. Huang, Supramolecular structures of peptide assemblies in membranes by neutron off-plane scattering: method of analysis, Biophys. J. 77 (1999) 2648–2656.
[25] L. Yang, T.M. Weiss, R.I. Lehrer, H.W. Huang, Crystallization of antimicrobial pores in membranes: magainin and protegrin, Biophys. J. 79 (2000) 2002–2009.
[26] K. Matsuzaki, O. Murase, H. Tokuda, N. Fujii, K. Miyajima, An antimicrobial peptide, magainin 2, induced rapid flip-flop of phospholipids coupled with pore formation and peptide translocation, Biochemistry 35 (1996) 11361–11368.
[27] G.A. Olah, H.W. Huang, Circular dichroism of oriented α-helices. I. Proof of the exciton theory, J. Chem. Phys. 89 (1988) 2531–2538.
[28] Y. Wu, H.W. Huang, G.A. Olah, Method of oriented circular dichroism, Biophys. J. 57 (1990) 797–806.
[29] W.T. Heller, A.J. Waring, R.I. Lehrer, H.W. Huang, Multiple states of beta-sheet peptide protegrin in lipid bilayers, Biochemistry 37 (1998) 17331–17338.
[30] T.M. Weiss, L. Yang, L. Ding, A.J. Waring, R.I. Lehrer, H.W. Huang, Two states of cyclic antimicrobial peptide RTD-1 in lipid bilayers, Biochemistry 41 (2002) 10070–10076.
[31] H.W. Huang, Y. Wu, Lipid-alamethicin interactions influence alamethicin orientation, Biophys. J. 60 (1991) 1079–1087.
[32] Y. Wu, K. He, S.J. Ludtke, H.W. Huang, X-ray diffraction study of lipid bilayer membrane interacting with amphiphilic helical peptides: diphytanoyl phosphatidylcholine with alamethicin at low concentrations, Biophys. J. 68 (1995) 2361–2369.
[33] S.J. Ludtke, K. He, H.W. Huang, Membrane thinning caused by magainin 2, Biochemistry 34 (1995) 16764–16769.
[34] W.T. Heller, A.J. Waring, R.I. Lehrer, T.A. Harroun, T.M. Weiss, L. Yang, H.W. Huang, Membrane thinning effect by the β-sheet antimicrobial protegrin, Biochemistry 39 (2000) 139–145.
[35] F.Y. Chen, M.T. Lee, H.W. Huang, Evidence for membrane thinning effect as the mechanism for peptide-induced pore formation, Biophys. J. 84 (2003) 3751–3758.
[36] H.W. Huang, Action of antimicrobial peptides: two-state model, Biochemistry 39 (2000) 8347–8352.
[37] M.L. Longo, A.J. Waring, L.M. Gordon, D.A. Hammer, Area expansion and permeation of phospholipid membrane bilayers by influenza fusion peptides and melittin, Langmuir 14 (1998) 2385–2395.
[38] K. Matsuzaki, O. Murase, H. Tokuda, S. Fumakoshi, N. Fujii, K. Miyajima, Orientational and aggregational states of magainin 2 in phospholipids bilayers, Biochemistry 33 (1994) 3342–3349.
[39] B. Bechinger, Y. Kim, L.E. Chirlian, J. Gesell, J.-M. Neumann, M. Motal, J. Tomich, M. Zasloff, S.J. Opella, Orientation of amphipathic helical peptides in membrane bilayers determined by solid-state NMR spectroscopy, J. Biol. NMR 1 (1991) 167–173.
[40] F.M. Marassi, S.J. Opella, P. Juvvadi, R.B. Merrifield, Orientation of cecropin A helices in phospholipid bilayers determined by solid-state NMR spectroscopy, Biophys. J. 77 (1999) 3152–3155.
[41] S. Yamaguchi, D. Huster, A. Waring, R.I. Lehrer, W. Kearney, B.F. Tack,

M. Hong, Orientation and dynamics of an antimicrobial peptide in the lipid bilayer by solid-state NMR, Biophys. J. 81 (2001) 2203–2214.
[42] R.W. Glaser, C. Sachse, U.H.N. Durr, P. Wadhwani, S. Afonin, E. Strandberg, A. Ulrich, Concentration-dependent re-alignment of the antimicrobial peptide PGLa in lipid membranes observed by solid state 19F-NMR, Biophys. J. 88 (2005) 3392–3397.
[43] H.W. Huang, Elasticity of lipid bilayer interaction with amphiphilic helical peptides, J. Phys. II France 5 (1995) 1427–1431.
[44] W. Rawicz, K.C. Olbrich, T. McIntosh, D. Needham, E. Evans, Effect of chain length and unsaturation on elasticity of lipid bilayers, Biophys. J. 79 (2000) 328–339.
[45] W. Helfrich, Elastic properties of lipid bilayers: theory and possible experiments, Z. Naturforsch 28c (1973) 693–703.
[46] E. Gazit, A. Boman, H.G. Boman, Y. Shai, Mode of action of the antimicrobial Cecropin B2: a spectrofluorometric study, Biochemistry 33 (1994) 10681–10692.
[47] E. Gazit, A. Boman, H.G. Boman, Y. Shai, Interaction of the mammalian antibacterial peptide cecropin P1 with phospholipid vesicles, Biochemistry 34 (1995) 11479–11488.
[48] M. Schumann, M. Dathe, T. Wieprecht, M. Beyermann, M. Bienert, The tendency of magainin to associate upon binding to phospholipids bilayers, Biochemistry 36 (1997) 4345–4351.
[49] T.J. McIntosh, S.A. Simon, Area per molecule and distribution of water in fully hydrated dilauroylphosphatidylethanolamine bilayers, Biochemistry 25 (1986) 4948–4952.
[50] J.F. Nagle, S. Tristram-Nagle, Structure of lipid bilayers, Biochim. Biophys. Acta 1469 (2000) 159–195.
[51] W.C. Hung, F.Y. Chen, The hydrophobic–hydrophilic interface of phospholipid membranes studied by lamellar X-ray diffraction, Chin. J. Phys. 41 (2003) 85–91.
[52] H.W. Huang, F.Y. Chen, M.T. Lee, Molecular mechanism of peptide induced pores in membranes, Phys. Rev. Lett. 92 (2004) (198304 (1–4)).
[53] F.Y. Chen, M.T. Lee, H.W. Huang, Sigmoidal concentration dependence of antimicrobial peptide activities: a case study on alamethicin, Biophys. J. 82 (2002) 908–914.
[54] M.T. Lee, F.Y. Chen, H.W. Huang, Energetics of pore formation induced by antimicrobial peptides, Biochemistry 43 (2004) 3590–3599.
[55] D. Allende, S.A. Simon, T.J. McIntosh, Melittin-induced bilayer leakage depends on lipid material properties; evidence for toroidal pores, Biophys. J. 88 (2005) 1828–1837.
[56] M.T. Lee, W.C. Hung, F.Y. Chen, H.W. Huang, Many-body effect of antimicrobial peptides: on the correlation between lipid's spontaneous curvature and pore formation, Biophys. J. 89 (2005) 4006–4016.
[57] W.T. Heller, K. He, S.J. Ludtke, T.A. Harroun, H.W. Huang, Effect of changing the size of lipid headgroup on peptide insertion into membrane, Biophys. J. 73 (1997) 239–244.
[58] F. Brochard-Wyart, P.G. de Gennes, O. Sandre, Transient pores in stretched vesicles: role of leak-out, Physica (Amsterdam) 278A (2000) 32–51.
[59] P.H. Puech, N. Borghi, E. Karatekin, F. Brochard-Wyart, Line Thermodynamics: adsorption at a membrane edge, Phys. Rev. Lett. 90 (2003) (128304 (1–4)).
[60] E. Karatekin, O. Sandre, H. Guitouni, N. Borghi, P.-H. Puech, F. Brochard-Wyart, Cascades of transient pores in giant vesicles: line tension and transport, Biophys J. 84 (2003) 1734–1749.
[61] K. Olbrich, W. Rawicz, D. Needham, E. Evans, Water permeability and mechanical strength of polyunsaturated lipid bilayers, Biophys. J. 79 (2000) 321–327.
[62] H. Duchohier, G. Molle, G. Spach, Antimicrobial peptide magainin 1 from *Xenopus* skin forms anion-permeable channels in planar lipid bilayes, Biophys. J. 56 (1989) 1017–1021.